Nearest-Neighbor Backscattering Effects in Angle-Integrated Photoemission Spectroscopy of Core Levels

G. Margaritondo and N. G. Stoffel
Department of Physics, University of Wisconsin–Madison, Madison, Wisconsin 53706
(Received 15 January 1979)

We have measured the photomission intensity versus photon energy curves of the Sn $4d_{5/2}$ level in SnS and SnS_2 and the In $4d_{5/2}$ and Se $3d$ levels in InSe up to 110 eV above threshold. The structure observed in these curves is mostly due to nearest-neighbor backscattering. This raises the possibility of surface extended x-ray–absorption fine-structure experiments by photomission intensity measurements.

Photoelectron diffraction effects[1] have been recently observed in angle-resolved collection geometries by several authors.[2-4] A complete explanation of these effects requires detailed scattering calculations.[2,3,5] We present here evidence for a simpler kind of photoelectron diffraction effect observed in an angle-integrated collection geometry. We have measured the intensity of the Sn $4d_{5/2}$ peak in SnS and SnS_2 and of the In $4d_{5/2}$ and Se $3d$ peaks in InSe in the limited collection geometry of a cylindrical-mirror analyzer up to 110 eV above the photoionization threshold. The observed modulations in the intensity versus photon energy curves arise from processes in which the photoelectron wave is scattered by one of the nearest-neighbor atoms directly back into the emitting atom. Processes of this kind are responsible for the extended x-ray-absorption fine structure (EXAFS) observed above each x-ray absorption threshold.[6-8]

The EXAFS formulas are quite simple and this has been a crucial factor in the widespread applications of the EXAFS technique. If we assume only one kind of neighboring atom at a distance r from the emitting atom, the k-periodic factor in the absorption coefficient modulation is given by $\Delta\alpha \propto \sin[2kr+\varphi(k)]$, where k is the magnitude of the photoelectron k vector and φ is the *total* scattering phase shift.[9,10] Thus, $\Delta\alpha$ gives direct information about r without requiring a detailed theoretical analysis of the photoelectron diffraction processes. It has been emphasized[6] that this simplicity of the EXAFS formulas is the result of integrating over 4π steradians the angle-resolved photoemission intensity. This integration is automatically accomplished while measuring the absorption coefficient. In photoemission experiments, instead, the upper limit for the angular integration is 2π steradians and in most cases is more limited. This would seem to rule out the possibility of surface-sensitive EXAFS measurements by monitoring core-level photoemission peak intensities.[6] As a consequence the surface-EXAFS technique has been based on the detection of Auger electrons.[8] EXAFS-like oscillations in the photoemission yield have been reported in the past by Petersen and Kunz for the $L_{2,3}$ edge of Na,[11] but these results did not directly contradict the conclusions of Ref. 6 since they had been obtained in polycrystalline samples. Our present results show instead that simple, EXAFS-like modulations are present in photoemission intensity curves of core levels taken with a limited angular integration on single-crystal samples. Our results have been obtained on layer compounds, a somewhat intermediate case between the adsorbate monolayers considered in Ref. 6 and a bulk system. In InSe, for example, the first two Se atomic planes are separated by two In planes and therefore the system is similar to an ordered Se monolayer adsorbed on an In substrate.

We have employed samples cleaved *in situ* and pressure of $(4-8)\times10^{-11}$ Torr. The photon source was the uv/soft-x-ray beam line of the University of Wisconsin Synchrotron Radiation Center equipped with a grazing-incidence monochromator ("Grasshopper"). The photon beam reached the sample at an angle of 78° from its normal and with the electric vector of the radiation parallel to its surface.[12] The sample normal coincided with the axis of the double-pass cylindrical-mirror analyzer. Thus the collection geometry corresponded to averaging the emission over all azimuthal angles and over polar angles between 36.3° and 48.3° (resulting solid angle ~ 0.88 sr). The experiment consisted of measuring the total intensity of each core-level photoemission peak as a function of photon energy. The intensity has been corrected for the secondary electron background (by linear interpolation), for the spectral output of the monochromator and for the variation in time of the current in the storage ring. The photoelectron kinetic energy inside the sam-

ple and the corresponding k-vector magnitude have been estimated using the photon energy, the measured binding energy of the core level with respect to the top of the valence band and the energy gap. Figure 1 shows the results for the $j=\frac{5}{2}$ component of the Sn $4d$ spin-orbit doublet in SnS and SnS_2. Figure 2 shows the data for In $4d_{5/2}$ and for the (unresolved) Se $3d$ doublet in InSe.[13] All these photoemission intensity curves exhibit modulation up to 20–25% superimposed on a smoother k dependence of atomic origin.[14,15] Closer than 10–14 eV to threshold ($k \lesssim 1.6$–1.9 Å^{-1}) the modulation must be explained in terms of the conduction-band structure.[16] Above ~1.9–2 Å^{-1} the analysis of the modulation becomes more straightforward as we shall discuss now.

The distance in k of the most prominent maxima in Figs. 1 and 2 immediately suggests that they are related to nearest-neighbor backscattering. For example, maxima are found for SnS_2 at 1.85, 3.1, and 4.35 Å^{-1}, with a periodicity of ~1.25 Å^{-1} corresponding to a difference in electron optical path of ~5.05 Å, close to twice the Sn-S distance of 2.56 Å.[17] In SnS the maxima of the corresponding series are found at 1.95, 3.1, and 4.35 Å^{-1}, with a periodicity decreased by ~4% with respect to SnS while the Sn-S distance correspondently increases by 5% to 2.68 Å.[18] Similar series of peaks are found for the Sn-Sn distance in[17] SnS (3.45 Å) and in[18] SnS_2 (3.64 Å), and for the In-Se, In-In, and Se-Se distances in InSe (2.51, 3.16, and 4.17 Å, respectively[17]). The modulation in k space is not as simple as implied in the previous analysis because of k-dependent atomic phase shift.[10] To have more confidence in the above identification we now compare the atomic phase shifts deduced from the experimental data to calculated values. From the estimated position of the peaks indicated by the vertical lines in Figs. 1 and 2 and the known interatomic distances[17,18] we have determined the phase shifts shown in Fig. 3. Also shown in Fig. 3 are the phase shifts from the atomic scattering calculations of Fink available for 100 eV ($k \sim 5.1$ Å).[19] We would like to emphasize the following points. First, the k dependence of our experimental phase

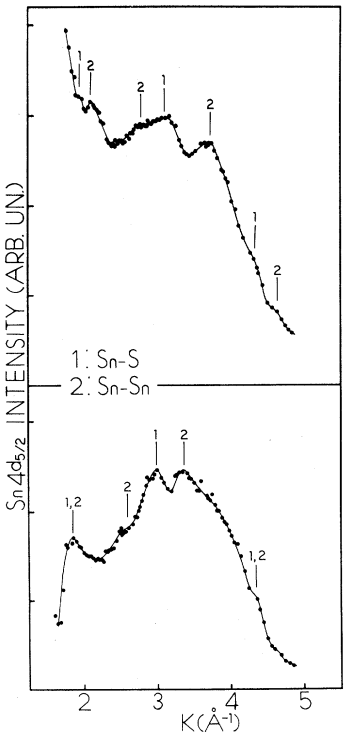

FIG. 1. The normalized intensity of the Sn $4d_{5/2}$ photoemission peak in SnS (upper curve) and in SnS_2 as a function of the k-vector magnitude. Two series of peaks have been identified in each curve. They correspond to Sn→S→Sn backscattering (series 1) and to Sn⇄Sn backscattering (series 2).

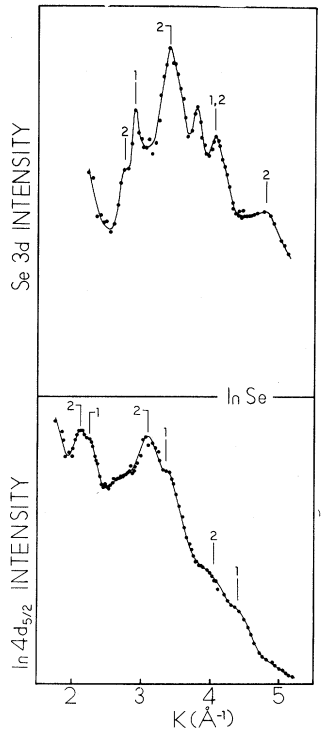

FIG. 2. The normalized intensity of the Se $3d$ photoemission peak (upper curve) and of the In $4d_{5/2}$ peak in InSe. For Se $3d$ the peaks of series 1 arise from Se →In→ Se backscattering and those of series 2 from Se ⇄ Se backscattering. For In $4d_{5/2}$ series 1 arises from In→ Se→ In backscattering and series 2 from In⇄ In backscattering.

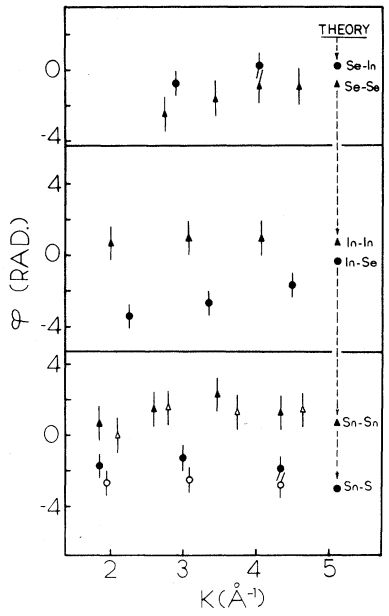

FIG. 3. The k dependence of the total phase shift deduced from our data (points with error bars) is consistent with the calculated values at 100 eV ($k = 5.12$ Å^{-1}, points without error bars). Top, phase shifts for Se $3d$ photoemission in InSe, caused by Se → In → Se backscattering (circles) and by Se ⇄ Se backscattering (triangles); middle, phase shifts for In $4d_{5/2}$ in InSe, In → Se → In backscattering (circles) and In ⇄ In backscattering (triangles); bottom, phase shifts for Sn $4d_{5/2}$ in SnS_2 (solid symbols) and in SnS (open symbols), due to Sn → S → Sn backscattering (circles) and to Sn ⇄ Sn backscattering (triangles).

shifts is consistent with the theoretical estimates at 100 eV. Second, the Sn ⇄ Sn and Sn → S → Sn phase shifts measured in SnS coincide with those measured in SnS_2 within the experimental uncertainty as implied by the "phase-shift transferability" in EXAFS.[10] Third, the dependence of φ on k for In ⇄ In backscattering is similar to that for Sn ⇄ Sn backscattering. This is consistent with the slow variation of the phase shift with the atomic number.[19] In summary, our phase-shift analysis supports nearest-neighbor backscattering as the main factor in the observed photoemission intensity modulation. Minor contributions from other scattering processes cannot be excluded in our data. For example, a phase-shift analysis indicates that the peak at 3.75–3.85 Å^{-1} in the upper curve of Fig. 2 is due to second-nearest-neighbor Se → In → Se backscattering with an interatomic distance of[17] 4.38 Å (the other peaks in this series could be responsible for the broadening of some of the nearest-neighbor peaks in Fig. 2). We have also examined possible scattering mechanisms without interference at the emitting atom (e.g., those involving a reciprocal-lattice vector normal to the surface) finding no evidence for their presence in our data.

In summary we have shown that a simple, EXAFS-like modulation of core-level photoemission intensity can be observed even with a limited angular integration. As to the possible practical consequences of this result a complete EXAFS analysis of our data to estimate interatomic distances[9] is made difficult by the underlying atomic effects. For core levels without nodes in the radial wave function, however, it should be possible to observe the modulation over an energy range more extended than ours making an EXAFS data analysis more feasible. Thus photoemission intensity measurements could be used in place of Auger intensity measurements in surface EXAFS experiments[8] to expand the possible applications of this technique.

We would like to thank M. B. Webb, M. Lagally, and J. E. Rowe for many useful discussions and suggestions. The friendly collaboration of J. H. Weaver and of the entire staff of the University of Wisconsin Synchrotron Radiation Center, which is supported by National Science Foundation Grant DMR-74-15089, has been of invaluable help in the experiment work. Thanks are also due to A. D. Katnani for his collaboration in the experiments and to F. Levy and H. Kasper for providing the samples. This work was supported by a Cottrel Research Grant of the Research Corporation and by the University of Wisconsin Graduate School Research Committee.

[1]A. Liebsch, Phys. Rev. B 13, 544 (1976).

[2]N. V. Smith, P. K. Larsen, and S. Chiang, Phys. Rev. B 16, 2699 (1977); D. P. Woodruff, D. Norman, B. W. Holland, N. V. Smith, H. H. Farrell, and M. M. Traum, Phys. Rev. Lett. 41, 1130 (1978).

[3]S. Kono, C. S. Fadley, N. F. T. Hall, and Z. Hussain, Phys. Rev. Lett. 41, 117 (1978); S. Kono, S. M. Goldberg, N. F. T. Hall, and C. S. Fadley, Phys. Rev. Lett. 41, 1831 (1978).

[4]S. K. Kevan, D. H. Rosenblatt, D. Denley, B.-C. Lu, and D. A. Shirley, Phys. Rev. Lett. 41, 1565 (1978).

[5]S. Y. Tong and N. Stoner, J. Phys. Rev. C 11, 3511 (1978).

[6]P. A. Lee, Phys. Rev. B 13, 5261 (1976).

[7]B. M. Kincaid and P. Eisenberger, Phys. Rev. Lett. 34, 1361 (1975).

[8]P. H. Citrin, P. Eisenberger, and R. C. Hewitt, Phys. Rev. Lett. 41, 309 (1978); A. Bianconi and R. Z.

Bachrach, Phys. Rev. Lett. 42, 104 (1979).
[9]P. A. Lee and G. Beni, Phys. Rev. B 15, 2862 (1977).
[10]P. H. Citrin, P. Eisenberger, and B. M. Kincaid, Phys. Rev. Lett. 36, 1346 (1976).
[11]H. Petersen and C. Kunz, Phys. Rev. Lett. 35, 863 (1975).
[12]Because of the symmetry of the initial states, the photon polarization does not play a major role in the analysis of our experimental data.
[13]Experiments have also been carried out for the $j=\frac{3}{2}$ component of In 4*d* and of Sn 4*d*. The intensity modulations discussed here were similar for these peaks and for their $j=\frac{5}{2}$ partners shown in Figs. 1 and 2. Differences between the $j=\frac{5}{2}$ and the $j=\frac{3}{2}$ intensity versus energy curves have been found to exist for the atomic background to which the modulations are superimposed and they will be discussed elsewhere.
[14]G. Margaritondo, J. E. Rowe, and S. B. Christman, Phys. Rev. B 19, 2850 (1979).
[15]U. Fano and J. W. Cooper, Rev. Mod. Phys. 40, 441 (1968).
[16]N. G. Stoffel and G. Margaritondo, unpublished.
[17]R. W. G. Wyckoff, *Crystal Structures* (Interscience, New York, 1964), Vol. 2.
[18]A. P. Lambros, D. Gerales, and N. A. Economou, J. Phys. Chem. Solids 35, 537 (1974).
[19]D. Gregory and M. Fink, At. Data Nucl. Data Tables 14, 39 (1974). Because of the slow variation of the phase shift with the atomic number, in our estimates we have employed Cd ($Z=48$) instead of In ($Z=49$) and Sn ($Z=50$), Br ($Z=35$) instead of Se ($Z=34$), and P ($Z=15$) instead of S ($Z=16$). The phase shift for the 180° scattering at the neighboring atom has been approximated with the calculated value for 178° scattering.

Photoacoustic Effect in Solids

C. L. Cesar, H. Vargas, J. A. Meyer, and L. C. M. Miranda
Instituto de Física, Universidade Estadual de Campinas, 13100 Campinas, São Paulo, Brazil
(Received 6 December 1978)

A quantitative derivation is presented for the production of the acoustic signal in a photoacoustic cell, taking into account the finite surface thermal resistance of the solid.

The photoacoustic (PA) spectroscopy has proved[1-6] to be an extremely useful tool for studying absorption spectra of crystalline, powdered, and amorphous solids as well as biological materials and liquids. In this Letter we develop the theory for the PA signal of a solid, taking into account, however, the surface thermal resistance of the sample. Our approach follows closely that of Rosencwaig and Gersho[2] (RG) and we refer to their work for further details.

Consider a simple cylindrical cell of diameter D and length $L=l+l_b+l_g$. The sample is considered to be in the form of a disk having diameter D and length l. A sinusoidally chopped monochromatic light with wavelength λ is incident on the solid with intensity $I=I_0(1+\cos\omega t)/2$, where I_0 is the incident monochromatic light flux and ω is the chopping frequency. We further assume that the gas and the backing materials are not light absorbing. We define the following parameters: k_i, thermal conductivity of material i; c_i, specific heat of material i; ρ_i, density of material i; $\alpha_i=k_i/\rho_i c_i$, thermal diffusivity of material i; $a_i=(\omega/2\alpha_i)^{1/2}$, thermal diffusion coefficient of material i; $\mu_i=1/a_i$, thermal diffusion length of material i; β, optical absorption coefficient of the solid sample. Here, the subscripts $i=s$, g, or b, denote the sample, gas, or backing material, respectively. Let $\varphi_i(x,t)$ denote the temperature in material i relative to ambient temperature (T_0) due to the light into heat conversion process. By neglecting the heat losses by radiation at the lateral surfaces (the inclusion of linear heat losses can easily be done), the temperature in cell obeys the same thermal diffusion equations as those of RG theory.[2]

The real part of $\varphi_g(x,t)$ is, of course, the solution of physical interest. This, in turn, is obtained by solving the thermal diffusion equations together with the appropriate boundary conditions. In the RG (Ref. 2) and other theories[3-5] the boundary conditions are temperature and heat-flux continuity at the sample boundaries $x=0$ and $x=-l$, together with the constraint that the temperature at the cell walls is at ambient temperature [i.e., $\varphi_g(x=l_g,t)=\varphi_b(x=-l-l_b,t)=0$]. This latter constraint is a reasonable assumption for metallic cell walls. On the other hand, the condition of temperature continuity at the faces $x=0$ and $x=-l$ is a very restricting one. In the general case, temperature continuity at the face of two bodies is only valid for very intimate contact, such as a soldered joint.[6] In all other cases, even for optically flat surfaces pressed lightly together, heat transfer between two media takes place largely by the linear heat-transfer mechanism,